

Grey Owl UAS Design, Development and Verification

2014 AUVSI Student UAS Competition



Abstract

This document describes the design, development and verification of the Grey Owl system, as developed by the Technion Aerial Systems (TAS) team. The team consists of members from the Aerospace Eng. and Computer Science faculties. For its first participation in the AUVSI Student UAS competition, the team has designed and manufactured its own custom airframe, suited for the competition's missions and integrated it with full autonomous capabilities, a high quality stabilized imaging payload and reliable, independent communications to the Mission Ground Station (MGS), while keeping safety a foremost priority through the entire process. With its main goal to assist the fire containment efforts, the Grey Owl UAV is thoroughly designed and tested to withstand high velocity winds while providing real time intelligence, surveillance and reconnaissance (ISR).

Table of Contents

1	System Engineering Approach.....	3
1.1	Mission Requirements Analysis.....	3
1.2	Design Rationale.....	3
1.3	Expected Performance	3
1.4	Programmatic Risks and Mitigation Methods.....	4
2	UAS Design Description.....	4
2.1	Airframe.....	4
2.2	Autopilot.....	10
2.3	Payload.....	12
2.4	Target Identification.....	14
2.5	Mission Ground Station (MGS).....	17
2.6	Air Drop Task	17
3	Flight Testing, System Verification & Airworthiness	18
3.1	Mission Task Performance.....	18
3.2	Payload System Performance.....	19
3.3	Guidance System Performance	19
3.4	Evaluation Results	19
4	Safety Considerations / Approach.....	19
4.1	Specific safety criteria.....	19
4.2	Safety risks and mitigation methods	20

1 System Engineering Approach

The design, development and verification of the Grey Owl system, consisting of vast engineering disciplines, while meeting the schedule and desired system maturity required:

- Detailed work plan.
- Continuous risk assessment and minimization – both safety risks and development risks.
- Integration of engineering know-how with RC models practice.
- Combination of analysis and simulations with extensive (ground and flight) testing.
- Ongoing participation of manufacturer and operator in the development process.

1.1 Mission Requirements Analysis

The competition consists of two primary tasks and 8 secondary tasks, each broken into specified parameters with thresholds and objectives. In order to properly determine the system's design, Mission Requirements Analysis is compulsory:

- a. Autonomous Flight Task – Primary – Overfly waypoints in a certain order at a specified location and altitude.
- b. Search and Identify Targets – Primary – Search for unknown amount of alphanumeric targets of different shape, size, color and orientation. Arrange the letters to decode a secret message.
- c. Automatic Detection, Localizing and Classification – Develop algorithm which performs automatic detection and identification of potential targets.
- d. Actionable Intelligence - Provide complete and accurate information of a target in real time during flight.
- e. Off-Axis Target – Identify a target located outside of the no-fly-zone boundary without crossing it.
- f. Simulated Remote Information Center.
- g. Emergent Target – Search for and identify a human (dummy) target “last seen” at a known coordinate (given before takeoff).
- h. Interoperability – Provide real-time position of the UAV to an external system supplied during the competition.
- i. IR Search – Identify a target outlined by a heated wire using an infrared sensor.
- j. Air Drop – Release an Egg/Ribbon projectile so that it lands within a specified target area.

1.2 Design Rationale

After analyzing the competition's requirements, the team had defined several goals:

a. Designing a lightweight and durable aircraft.	b. Using a two-engine configuration.
c. Designing an aircraft which is user friendly.	d. Conducting an autonomous flight.
e. Orientation and autonomous target identification.	f. Real time data transfer from the aircraft to the Mission Ground Station.
g. Identifying a target that is located outside the permitted fly zone [without leaving it].	h. Identifying a target which wasn't predefined.
i. Performing an Air Drop mission.	

Table 1 – The team's goals for the competition

1.3 Expected Performance

After reviewing the competition rules, the following requirements and expected performance were established:

- Fully autonomous flight capabilities with manual override (safety)
- Autonomous target acquisition capabilities
- Separate communication protocols: Imaging relay, autopilot control and safety pilot control
- Long range: Flight Control function
- High-Speed: Target Acquisition function
- Standard 8ch remote controller (safety requirement)
- 40 minutes of flight time without replacing batteries
- Maximum takeoff weight < 12 kg
- Maximum airspeed < 100 KTAS
- Stall velocity ≈ 20 KTAS

- Altitude range during flight: 100-750 ft AGL
- Customized UAV (Unmanned Aerial Vehicle) suited for the competition's missions
- Survivability

1.4 Programmatic Risks and Mitigation Methods

In the design process of such a system there are many risks that should be considered and handled beforehand. The following table presents the possible risks and a solution for each one:

Risk	Solution
Crashes and damage to the UAV	Simplify design and build two complete UAVs
Communication issues between the UAV and the ground post	Redundancy in primary control, allowing for transition from autopilot mode to manned control from the ground
Issues recognizing targets using the algorithm due to unexpected conditions	Execution of the experiments in different weather, vision and background conditions and thus improving the algorithm
Lack of communication between members of the group	Execution of many experiments in order to improve team work
Power outage	Presence of reserve batteries at the ground post and returning the UAV to "base" to change batteries during the competition if needed
Vibrations and instability of the camera	Shock absorbing mount for the gimbals and aerodynamic nose cover to the camera
Minor damage to the UAV fuselage	Simplify design and equipping the ground post with materials and components that will enable a quick fix before returning to action

Table 2 – Programmatic risks and mitigation methods

2 UAS Design Description

2.1 Airframe

The conceptual design process of an aerial system begins with an assessment of the main tasks it will be required to complete and an initial determination of the aircraft's basic configuration, size and weight. Once these are decided upon and the propulsion system is chosen, the preliminary design process can begin.

This process entails the narrowing of more specific design elements, such as the location of all major sub-systems and the general shape of the aircraft, dictated by its wing style and location, tail style, and fuselage contour.

The Air frame's main configuration had to meet 3 main objectives:

1. Flexibility – allowing large variety of systems to be incorporated in the UAV.
2. Simplicity – for fast manufacturing and system integration as result of a tight schedule.
3. Efficiency – both aerodynamic and structural to allow for best payload to airframe weight ratio.

Three options were examined for the main aircraft configuration: conventional, canard and flying wing.

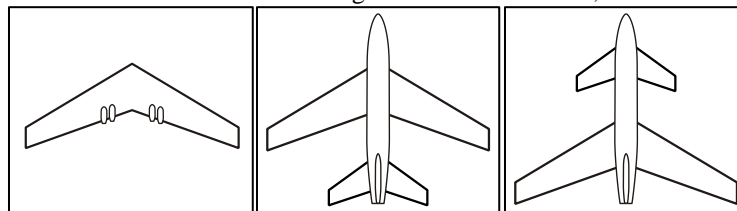


Figure 1 - Flying wing, conventional and forward tail (canard) configurations

Although the flying wing has a better lift to drag ratio, the conventional and canard configurations allow for much easier system integration in their main hull and pose lesser development risks. The contribution of the forward tail (canard) to the aerodynamics and controllability of the airframe was not considered ample enough to compensate for the pilot's and team's lack of experience flying and integrating the configuration. Therefore, a conventional airframe was selected.

Once the aircraft's main configuration was established, the camera location was chosen to allow for maximum flexibility in camera size and minimum structural penalty. Out of two locations examined (the nose and the

undercarriage of the UAV), the nose camera was chosen to allow for minimal structural penalty, easy integration of different cameras and greater opening for the camera which allows for wider field of view.

Three locations were considered for the engines: front (tractor), back (pusher) and wings (twin engine). The tractor engine was ruled out due to the camera's location. A pusher propeller has a lower efficiency due to the downwash induced by the wing and some shielding by the fuselage. The pusher configuration also invokes cooling issues and needs greater ground clearance or a double boom style fuselage (both having further aerodynamic and structural penalties). From this reasoning, twin engines located on the wings were chosen. The twin engines configuration has another advantage/drawback, single engine failure and the resulting yawing. This was taken into account in the aerodynamic analysis performed later on.

Wing geometry has a low effect over the overall efficiency of a high aspect ratio wing, therefore the dominating factor in choosing the geometry proved to be the stall characteristics of the wing, its weight, and its ease of manufacture. The three possibilities being elliptical tapered and rectangular wing, where the elliptical wing is the most aerodynamically efficient and the rectangular is the best in terms of stall characteristics and ease of manufacture, the rectangular wing was chosen.

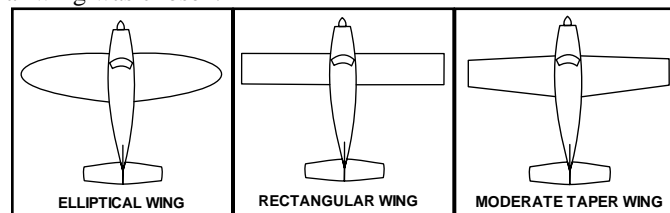


Figure 2 - Wing geometries (Elliptical, Rectangular and Tapered)

Location of the wing here is referring to the wing's position relative to the fuselage in terms of top, middle and bottom. The factors here are the induced dihedral inflicted on the wing due to high or low wing, the added ground clearance required for a lower wing, structural penalty due to the "wing box" required by a middle or top wing and the ease of transportation (disassembling and reassembling) of the UAV.

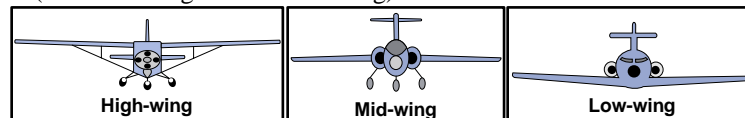


Figure 3 - Wing locations: Top, Middle and Low wing

Assessing all the above factors for each wing location, top location was decided upon as this would allow for the smallest landing gear, reducing the overall weight and drag of the airframe while allowing easy transportation of the UAV. The wing box required by this location would also double as the battery compartment, allowing easy access and eliminating the extra reinforcement needed for this structure.

Fuselage style and shape were chosen to allow for the maximum flexibility in system integration. The main rectangular hull is suitable for the rectangular batteries, flight controller and rectangular payload while ensuring great structural integrity and small aerodynamic penalty in comparison with a round shape. A double boom and pod style fuselage were also considered but were abandoned due to longer manufacturing process (double boom style) and inferior flexibility (pod style)



Figure 4 - Pod style fuselage



Figure 5 - Double boom



Figure 6 - Main hull

Parallel to analysis of the system's configuration, an evaluation of the UAV's structure was conducted. Several options were considered, which resulted in a graphite-epoxy fuselage along with balsa-foam wing and tail. A graphite-epoxy structure provided the greatest manufacturing flexibility given the decision to build two complete UAVs, but was deemed impractical for the wing due to the complexity and the project's work plan.

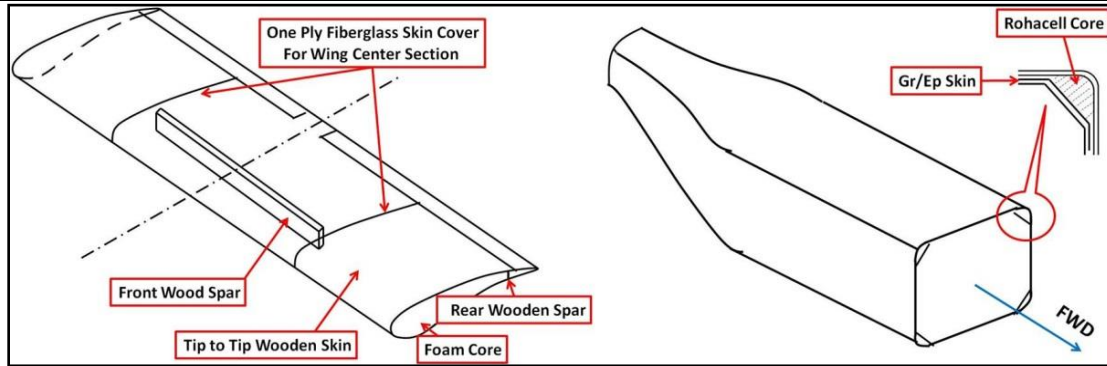


Figure 7 - Airframe structure

After performing structural analysis based on shape and material limitations, an MDF (Medium-Density Fibreboard), CNC-cut (Computer Numeric Control) mold was designed and manufactured on campus.



Figure 8 - Fuselage Lay- Up and manufacturing Tool

Nose Design and Camera - Gimbal Integration

The Nose and the Camera integration were design based on the following requirements and considerations:

- Aerodynamic shape nose for minimum drag
- Stabilized Camera with clear field of view
- Nose internal shape will allows for camera and gimbals full operation with adequate clearances
- No additional optical cover for the camera to ensure minimum image distortions
- Nose lower contour shape was designed to reduce turbulence affecting the camera
- Easy and quick removal of the nose for checking and maintenance

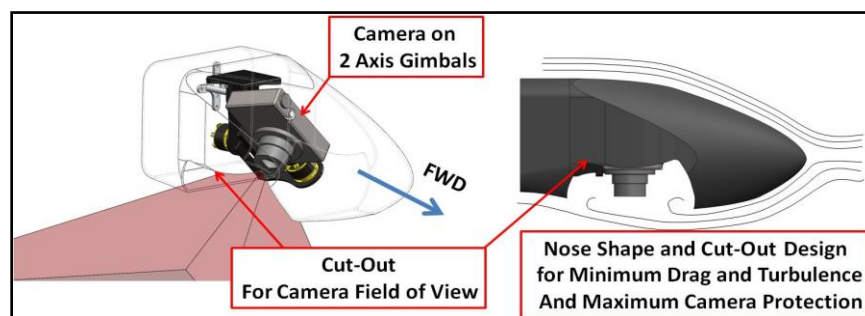


Figure 9 - Nose design and camera integration

The aircraft's stability was analyzed and its center of gravity was set after a review of all system components' weights & positions in an iterative process.

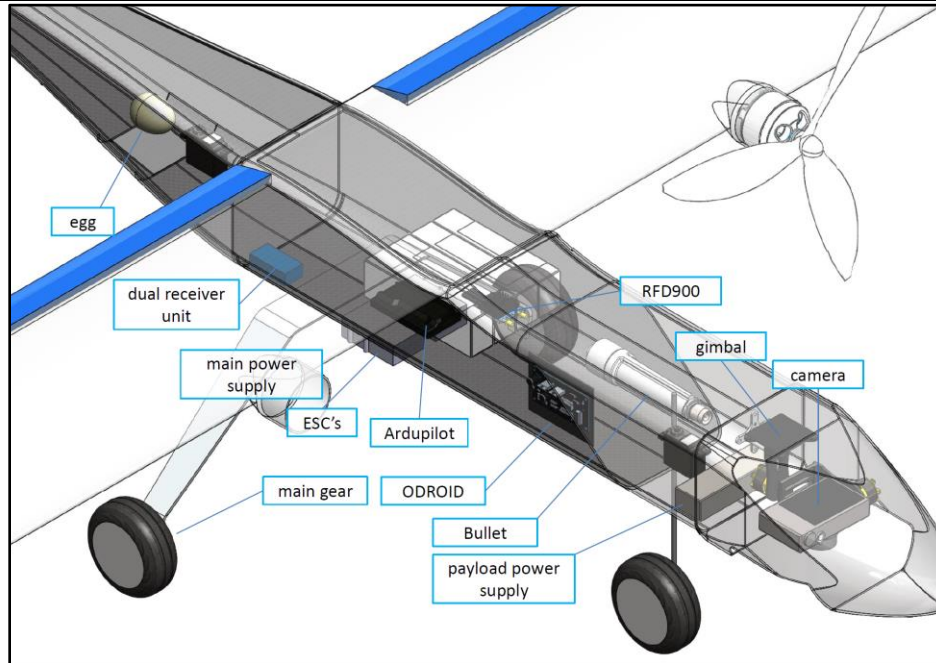


Figure 10 – Systems Internal Lay-Out Arrangement

The C.G location was found at station 506.65[mm] which is 55% MAC and gives 15.2% Positive Stability margin. Stability analysis was conducted in order to ensure longitudinal ($C_{M\alpha} < 0$) and lateral ($C_{N\beta} > 0$) stability.

$C_{L\alpha}$	5.5	$C_{M\alpha}$	-1.8	C_{Mq}	-26.2	$C_{N\beta}$	0.110
$C_{Y\beta}$	-0.230	$C_{l\beta}$	-0.012	C_{Np}	-0.005	C_{lr}	0.031
C_{lp}	-0.540	C_{Nr}	-0.110	C_{Yr}	0.230	C_{Yp}	-0.010

Table 3 - Stability Derivatives

Propulsion Type - (Piston vs. Electric)

The first step in choosing the propulsion system is choosing the type of propulsion, and so a comparison was made between the two most common propulsion configurations today: electric and piston.

The electric configuration was chosen due to its low price, ease of installation, light weight, negligible vibrations [which would affect the target identification process] and high reliability.

Design Goals

- Propulsion system that can handle a diversity of airspeeds while achieving the highest airspeed needed for all the various mission tasks.
- Long endurance flight and sufficient batteries for at least 40 minutes of moderate flight.
- Required Power loading: 110-165 W/Kg.

The aircraft weight is 10.4 [Kg] , from here the power was calculated:

$$P = \text{Weight} \cdot \text{Power loading} \rightarrow 1100 [w] < P < 1650 [w]$$

Several motors were examined and compared through various categories such as: weight, reliability, performance and motor temperatures.

Static thrust tests were conducted in order to validate theoretical models. Comparisons were made between several motors to increase the sample size, all results were checked against the specifications provided by the manufacturers to verify each product's reliability and performance.

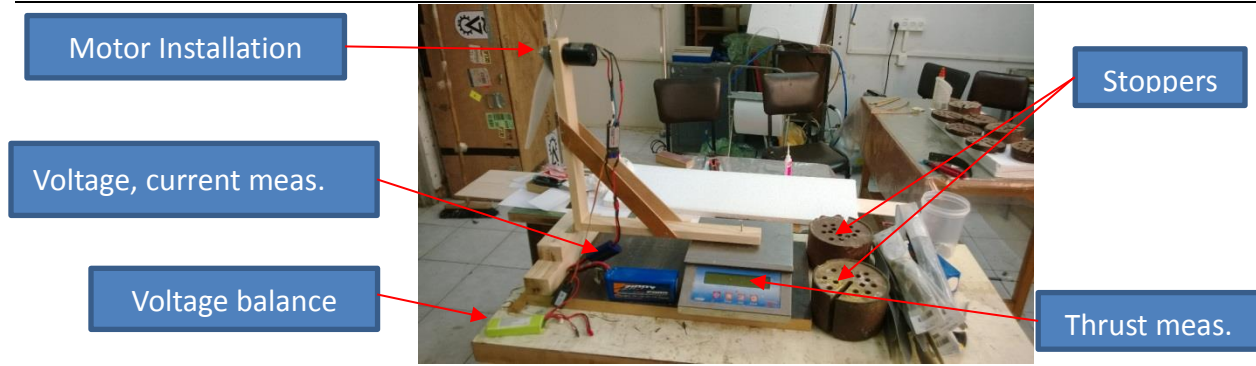


Figure 11- Static thrust testing

Propulsion system components

The motor selected according to the considerations presented above was "Plettenberg orbit 25-16".



Figure 12 - Plettenberg orbit 25-16

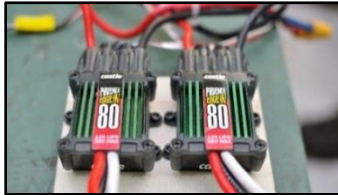


Figure 13 - Creations, Phoenix Edge HV80



Figure 14 - e-flite 5000mAh 4S 14.8V 30C LiPo

The Orbit 25-16 is a brushless out-

runner electric motor from the German manufacture Plettenberg Motors. This motor has a velocity constant of ~ 590 and an electric burst power of 1860 [W].

The next step was choosing an electric speed controller (ESC). The Phoenix Edge HV80 from Castle Creations was chosen for its compatibility with the selected motor and reliability, having high voltage capabilities (up to 44.4 [V]) and continuous current transfer up to 80 [A].

The propulsion configuration was completed by choosing batteries capable of sustaining system operations during the mission. The selected batteries are e-flite 5000mAh 4S 14.8V 30C LiPo. They are characterized by low internal resistance, high current load capability (max continuous current of 150A), good voltage stability and a long life span. They weigh 500 grams, which is relatively light compared to other competing batteries manufacturers.

Performance Evaluation

The graph below was drawn based on static thrust results, the motor efficiency can be obtained as a function of RPM. The motor max efficiency is 88.82% at an RPM of 7780, which is around the RPM the engines require to operate during straight and level flight and so provides a good estimate of motor efficiency.

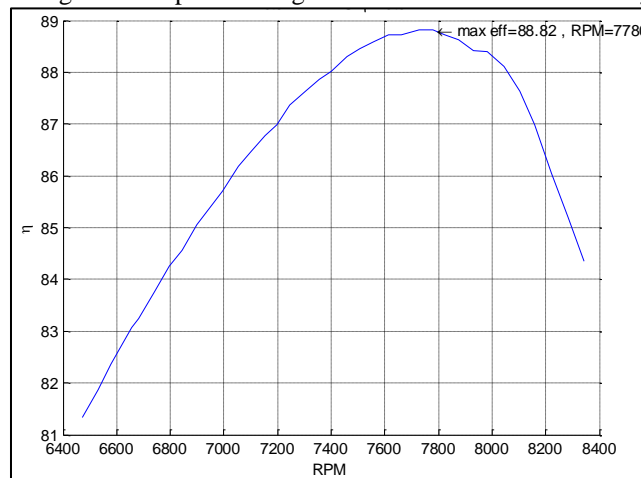


Figure 15 - Motor RPM Vs. motor efficiency

Propeller analysis was performed in a similar fashion, resulting in APC 17x10, which at an RPM of 7780 (direct drive) has an efficiency is about 0.76. The advancement ratio J at this efficiency and RPM is 0.66.

Once all components of the propulsion system were selected, the battery capacity was assessed using motors power requirement, efficiencies and the desired cruising speed of the UAV.

Aerodynamic Analysis

The airframe geometry was designed to meet the requirements defined by the team, and was done in several steps. Mainly, selecting the two-dimensional airfoil shape and selecting the three-dimensional wing, tail and fuselage geometry.

- Several airfoils, which were known to be compatible with the mission requirements, were examined.
- The top parameters for comparison were the aerodynamic efficiency and the lift coefficient in order to achieve minimum stall velocity.
- A Reynolds number of 5×10^5 was used based on initial assumptions of chord length and cruise velocity.

The improved aerodynamic characteristics of the Eppler 560 profile, combined with its high t/c ratio (16%) which enables a better load-carrying wing structure, led us to select the Eppler 560 profile. The symmetric NACA 0012 profile was chosen for both the vertical and horizontal stabilizers due to its recognized and proven performance in RC model practice, and its compatibility was verified under stability analysis.

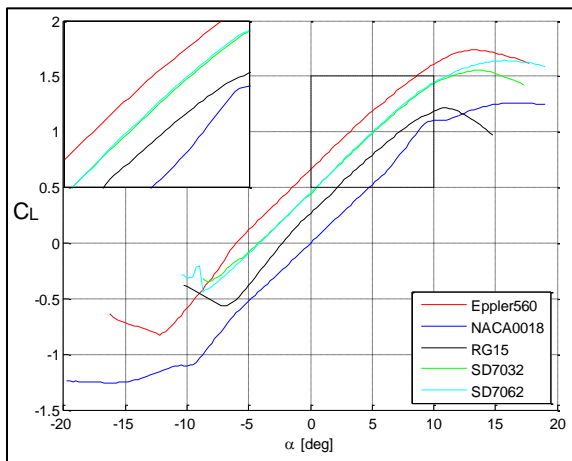


Figure 16 – Lift coefficient vs. Angle of attack for $Re = 5 \cdot 10^5$

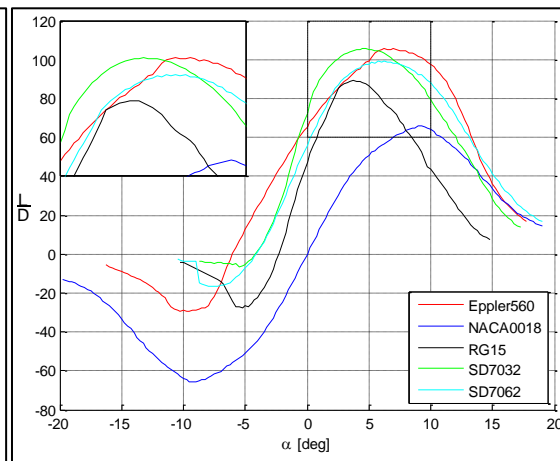


Figure 17– Aerodynamic efficiency vs. Angle of attack for $Re = 5 \cdot 10^5$

Once the two-dimensional airfoil was chosen, an analysis of the three-dimensional aircraft geometry was conducted. For the purpose of preliminary sizing, aspect ratio, wing load and tail volume were chosen to ensure a stable aircraft which will satisfy endurance, velocity and wind resistance requirements along with limitations on the wing span from a practical manufacturing perspective.

With the twin-engine configuration, it is important to verify that a single engine failure will not cause the aircraft to crash. A margin of safety was introduced to the lateral stability analysis, thus resulting in a larger tail. Afterwards, flight tests and simulated single engine failure confirmed the analysis and the UAV ability to land with a single engine.

All dimensions were chosen in an iterative process, based on the system's weight and the surface density of the wing and tail. The selected dimensions were tested using XFLR5 and were corrected according to this analysis to achieve the desired static stability margin.

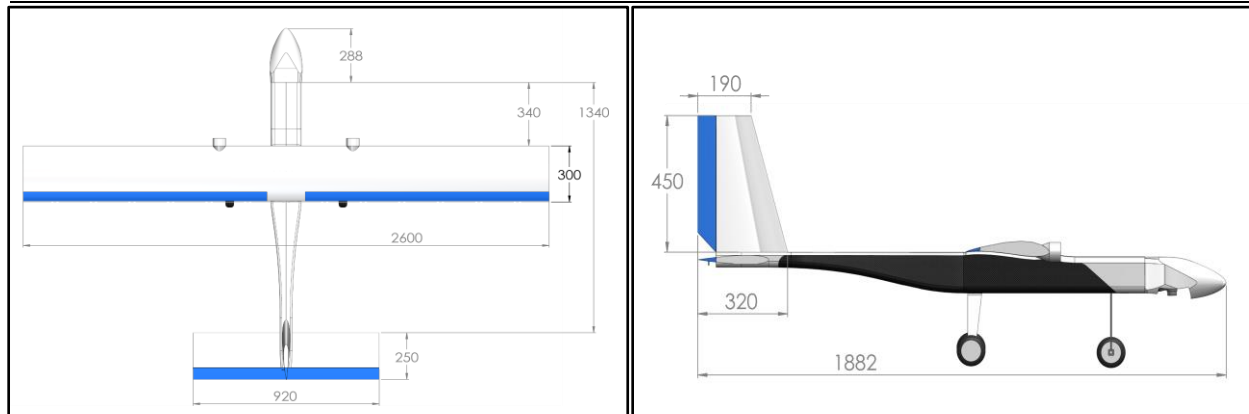


Figure 18 - UAV's Dimensions

Design Characteristics:

Main Wing		Vertical Stabilizer		Horizontal Stabilizer	
Airfoil	Eppler 560	Airfoil	NACA 0012	Airfoil	NACA 0012
Span	2.6[m]	Span	0.45[m]	Span	0.92[m]
Area	0.78[m ²]	Area	0.11[m ²]	Area	0.23[m ²]
Aspect Ratio	8.7	Aspect Ratio	1.8	Aspect Ratio	3.7
Aircraft Dimensions		Figures of merit		Propulsion System	
Weight	10.4[kg]	Wing Loading	13.33 $\frac{kg}{m^2}$	Power	1650[W]
Length	1.8[m]	Power Loading	159 $\frac{watt}{kg}$	Motors	2X Plettenberg orbit 25-16
Width	2.6[m]	Load Factor	3.5	Batteries	5X 5000mAh 14.8V LiPo
Height	1.05[m]			Prop. Size	17X10

Table 4 – Structural Characteristics/Capabilities

2.2 Autopilot

In order to incorporate fully autonomous capabilities to the airframe while minimizing safety and development risks, the autopilot system had to fulfill the following requirements:

- Proven Hardware & Software – Used worldwide in the unmanned drones community and especially in the AUVSI Student UAS competitions.
- Pilot's manual override – Possible at all stages of flight, directly from the pilot's radio controller.
- Easy sensors integration – "Plug & Play" Air Data, Attitude and Heading reference system (ADAHRS), Navigation and propulsion monitoring sensors.
- 2-way long range radio communication capable – Delivering real time telemetry and receiving flight plan & commands from the ground operator.
- Dedicated ground control application.
- Vast functional capabilities – Waypoint navigation, midair re-tasking, autonomous takeoff & landing and designated mission scripting.
- Small and lightweight airborne hardware, with low power consumption and no special cooling requirements.
- Affordable overall solution.

After thorough examination of Commercial off the Shelf (COTS) systems and complementary products, two main boards were considered, the ArduPilot Mega (APM) 2.6 and the Pixhawk. Finally, the autopilot of choice was the ArduPilot Mega 2.6 in the following configuration:

Component	Application	Sensors
ArduPilot Mega 2.6	Autopilot	<ul style="list-style-type: none"> •Invensense's 6 DoF Accelerometer/Gyro MPU-6000 •Measurement Specialties' MS5611-01BA03 barometric sensor
3DR uBlox GPS / Compass Kit	Navigation	<ul style="list-style-type: none"> •uBlox LEA-6H GPS module •Honeywell HMC5883L Magnetometer
RFD900 +2xQuarter wave antennas, 2.1dBi	Communication	•N/A
APM 2.6 Airspeed Sensor Kit	Air Data	•freescale MPXV7002 differential pressure sensor
APM Power Module	Autopilot Power Supply & Propulsion Monitoring	•APM Power Module
Futaba R6008HS 8-ch receiver	Manual Control	•N/A
Savox SC-1258TG digital servos	Actuators	•N/A

Table 5 - Grey Owl flight control & navigation configuration

Although the APM 2.6 and the Pixhawk autopilot share the same ground tool, "Plug & Play" components and desired functionalities, the APM architecture, though being old, has proved itself over the years as a reliable platform, hardware and software alike.

In order to allow sufficient autonomous flight control and navigation capabilities, the UAV had to incorporate real time absolute navigation solution with a <3m Circular Error Probability (CEP), interference resistive magnetometer with <4° compass heading error and an airspeed sensor (Pitot tube) with <2.5% airspeed error. With the above Pitot tube installed at the nose of the UAV, the external 3DR uBlox kit behind the wing alongside its built-in Inertial Measurement Unit (IMU) and barometric sensor, the autopilot is able to calculate its attitude, location, altitude, heading and bearing in a manner both efficient and reliable for the missions at hand.



Figure 19: Autopilot Configuration

As far as communication, The UAV's graphite-epoxy fuselage required robust communication modules and proper installation design. With its two antenna design and hi-power level, the RFD900 provides exceptional range and, more importantly, better signal integrity than any other communication modules examined for the APM. The same goes for the manual controller, where a Futaba Advanced Spread Spectrum Technology (FASST) receiver, equipped with two antennas for robust communication, was installed as a safety measure to be used by the pilot if necessary. A fast response, quick acceleration and excellent holding power required the use of digital servos, while the need for high survivability required a durable gear. After analyzing the maximum loads required for the Grey Owl UAV and examining several servo models, the Savox titanium gear digital servos were chosen.

2.3 Payload

Grey Owl's payload can be broken into 5 components:

- | | |
|---|---------------------------------------|
| 1. High Speed Communication Modules (Bullet M2 & M5). | 4. Gimbal (custom made for the S110). |
| 2. Onboard Computer (ODROID-XU). | 5. INS / GPS (VECTORNAV VN-200). |
| 3. Camera (Canon Powershot S110). | |

These components working together are able to communicate to the Mission Ground Station via four wireless links: the primary 2.4 GHz radio control transmitter, the 900 MHz autopilot Mission Ground Station, 5.8 GHz imagery Mission Ground Station and the 2.4GHz router in repeater mode for SRIC task. These Communications systems were chosen with the following considerations in mind:

- An operational range of 1.5km (taken according to map details from the 2010 AUVSI Student UAS competition and review of the competition site) with two payload data links – main (operational) and backup (standby).
- A system that can work in an environment in which multiple teams are allowed to transmit RF communications at the same time.
- Avoiding cross interference of systems.
- Overcoming Graphite-Epoxy disruptions in transmission.
- Choosing the lightest and smallest antenna while maintaining a strong signal within range (while considering weather conditions on the field site according to previous forecasts).
- Data transfer speed of at least 20 Mb per second for the Payload-MGS link.
- Short connection time.
- Reliable and simple-to-operate system.



Figure 20 - The 1.5[km] range of operation of the data links

Components	Details	Description
UBIQUITI Bullet M5-HP, 5.8GHz Wi-Fi (UAV)	6 [Watt] Powered over Ethernet 5 [dBi]	Provide the ability to gather information from the UAV to the MGS with a range of up to 27Km, satisfying results in a range of 1.5km. Adds an additional 11 channels of communication, reducing the number of connections necessary on the airframe.
UBIQUITI NanoStation M5, 5.8 GHz Wi-Fi (MGS)	6 [Watt] Powered over Ethernet 11 [dBi]	
UBIQUITI Bullet M2-HP, 2.4 GHz Wi-Fi (UAV)	6 [Watt] Powered over Ethernet 5 [dBi]	The router searches for its configured host Access Point. When an AP is found the Bullet automatically connects to the router using the specified security settings. The router also creates a secondary wireless network using the same settings as used in the host access point. Once connected, the router internally bridges all three interfaces: the host Access Point (AP), the secondary wireless network and the Bullet's Ethernet port. Once bridged, all clients on each interface appear on the same network subnet, allowing each communication to reach all clients.
UBIQUITI NanoStation M2, 2.4 GHz Wi-Fi (MGS)	6 [Watt] Powered over Ethernet 5 [dBi]	

*In case of a weak signal the SRIC data link can function as a backup link for the imagery link. This can be done at any time from MGS by changing the onboard Bullet to AP mode. In case of a link fail test, reconnection time is less than ten seconds.

Table 6 - Communication system components

Target Detection System

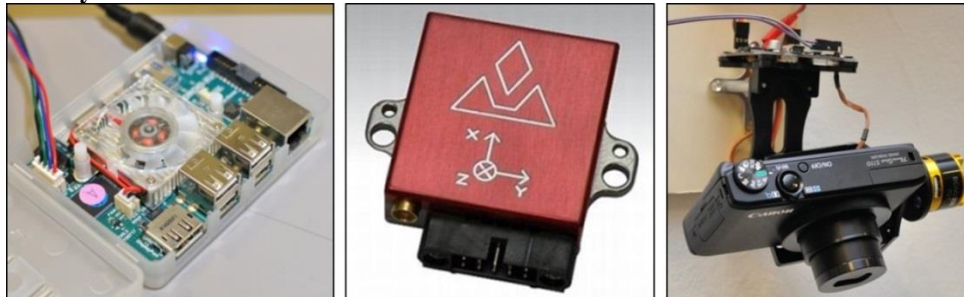


Figure 21 - Left to right: ODROID-XU Image processing platform, VectorNAV INS, Gimbaled Cannon S110

Computing platform

In order to provide powerful in-flight communication and image processing capabilities for target detection on the Grey Owl UAV it was decided to embed an ODROID-XU (Odroid). This system as seen in the left image of Figure 7 features an Exynos5 Cortex™-Arm A15 1.6 GHz quad-core CPU, USB & Ethernet connections and high speed eMMC storage while weighing 140 grams, measuring 98x74x24mm and maintaining a power consumption not exceeding 4 Ampere at 5 Volt (20 Watt). The Odroid supports various Linux distributions giving easy access to many of the tools used throughout the project (MySQL, Python, OpenCV, etc.). By taking advantage of the multicore nature of Odroid, the target detection algorithm is able to run in parallel using all four available cores. Furthermore the device can handle simultaneous high-speed wireless communication while also performing intensive disk read and write accesses.

Imaging and positioning systems

An extensive camera selection process was performed to find a camera with the right qualities for the UAV. The main factors considered were the need for high resolution imagery at a high global shutter speed with fully controllable software integration that was simultaneously small and light. A Galaxy S3 smartphone would have been ideal because of the device's multiple integrated sensors and powerful computing platform however the camera was determined to be rolling shutter and insufficiently controllable. A Raspberry PI unit coupled with a

camera module was identified as having poor image quality despite good resolution and computational abilities. An 8MP See3Cam module with USB 3.0 transfer was also considered however driver compatibility issues and board fragility meant that this camera was eventually abandoned. Similarly a USB3.0 PTGrey Grasshopper was initially tested but was both excessively expensive and suffered driver issues.

The camera that was eventually chosen was a 12MP Canon S110 Powershot. The camera is loaded with the Canon CHDK and combined with the chdkpt client application on the Odroid enables direct software based control of the camera's parameters and functionality including setting its optical zoom for a 32° horizontal field of view. The S110 can be seen sitting on the Grey Owl gimbal on the right most image of Figure 7. This is a custom built 2-axis brushless active gimbal system designed to stabilize the camera, remove roll and pitch and most importantly prevent image blur which might otherwise negatively impact the ability to identify targets.

In order to take high-quality position and orientation measurements for each captured image it was decided to include the VectorNav VN-200 Inertial Navigation System (INS). The INS unit, connected to the Odroid, is positioned on the gimbal next to the camera. This provides the camera's real time orientation, as well as GPS coordinates and altitude of the UAV. Clock synchronization for the camera-INS combination is performed by finding and compensating the average offset between capture time and storage time for a new image.

2.4 Target Identification

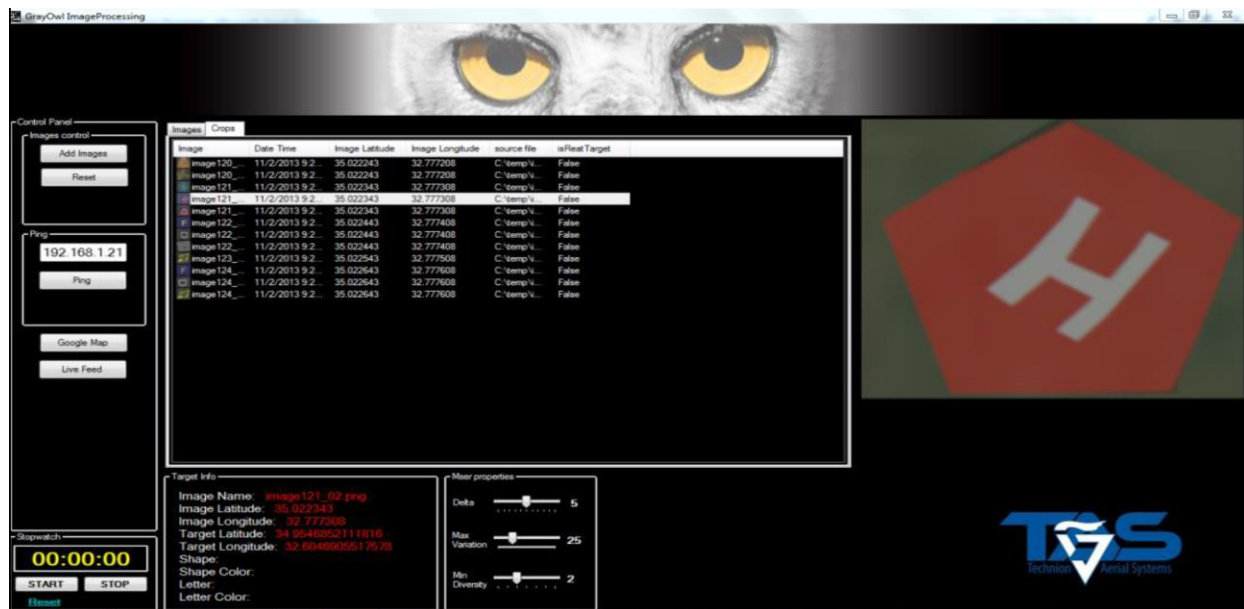


Figure 22 - Fully custom built Grey Owl AUV image processing GUI which mediates communication and target processing and display

The target identification consists of two main processing components: the airborne Odroid and the Mission Ground Station (MGS). Both computers take part in the image process workflow:

- Images are captured by the S110 camera and stored directly on the Odroid.
- Potential targets are identified using the Python OpenCV Maximally Stable Extremal Regions (MSER) interest point detector running on multiple Odroid cores in-flight.
- The MGS constantly polls the Odroid with HTTP requests and when available receives the following data: a down-sampled version of the original picture, image crops generated by MSER, an XML file for each image and image crops with the GPS location of the UAV at the time the image was captured together with the orientation of the camera.
- The MSER crops and positional data are processed by the MGS. Each crop is classified using a pre-trained Support Vector Machine (SVM) as being a target or non-target. Accepted targets are passed on to the target characteristic extraction algorithms.
- All the data is displayed in near-real time in a fully custom designed graphical user interface (GUI).

Initial target detection and localization

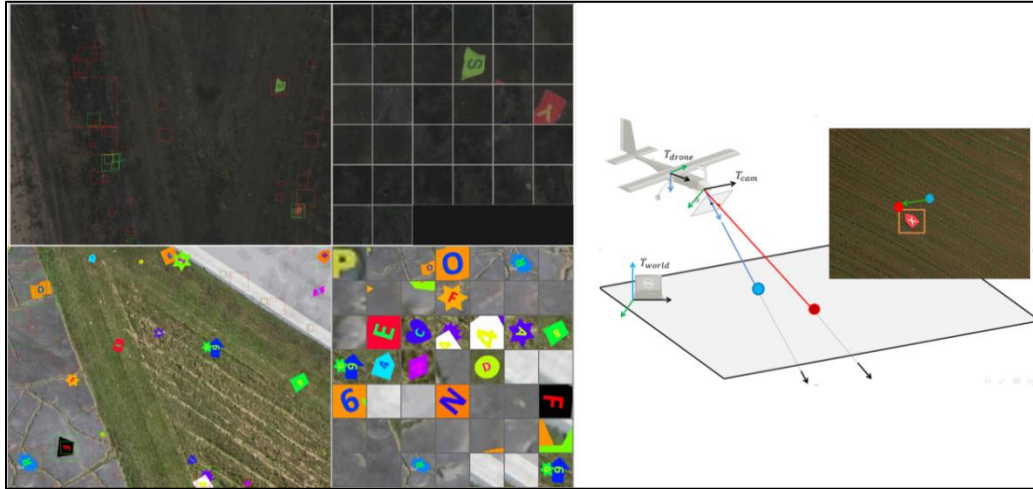


Figure 23 - Top left: Real flight image with a montage of the MSER detections. Bottom left: A simulated flight image with a montage of the MSER detections. Right: Axis setup for camera relative to MGS location.

The Odroid uses MSER to detect possible regions in which targets are located. These regions are then filtered according to overlap and proximity to one another to decide which regions of the image are likely to contain targets. The MSER parameters are chosen to provide high Recall and low Precision so as to minimize the risk of missing targets. A montage of the detected potential targets for a real flight and simulated flight can be seen in Figure 9. One of the critical mission objectives is to determine the accurate GPS location of each of the detected MSER targets. Our goal is to use the camera parameters (f, c_x, c_y), GPS location (CAM_{lon}, CAM_{lat}) and orientation data of the camera ($R_{yaw}, R_{roll}, R_{pitch}$), along with the pixel position (u, v) of a target. We find the intersection between a ray from the camera through the target pixel in the image plane with the real world ground plane as shown in the right image of Figure 23. The altitude above ground level is denoted as Δh . The following describes this computation using all the information available to us:

Target offset in meters from current camera location:

$$\begin{pmatrix} \Delta x \\ \Delta y \\ 0 \end{pmatrix} = \begin{pmatrix} 0 \\ 0 \\ \Delta h \end{pmatrix} + \Delta h \cdot \begin{pmatrix} 1 & 0 & 0 \\ 0 & 1 & 0 \\ 0 & 0 & -1 \end{pmatrix} \cdot R_{yaw} \cdot R_{roll} \cdot R_{pitch} \cdot \begin{pmatrix} f & 0 & c_x \\ 0 & -f & c_y \\ 0 & 0 & 1 \end{pmatrix}^{-1} \cdot \begin{pmatrix} u \\ v \\ 1 \end{pmatrix}$$

Target GPS coordinates:

$$\begin{pmatrix} TARGET_{lon} \\ TARGET_{lat} \end{pmatrix} = \begin{pmatrix} CAM_{lon} \\ CAM_{lat} \end{pmatrix} + \begin{pmatrix} \Delta x / r_{polar} \\ \Delta y / (r_{equatorial} \cdot \cosd(CAM_{lon})) \end{pmatrix} \cdot (180/\pi)$$

Eliminating false positives

Classification of a crop to be a valid or non-valid target is done using a Support Vector Machine (SVM) with a linear kernel. We use a number of different features for describing each target for training the SVM. K-Means clustering on each RGB crop with $K=4$ is used to split the crop into several regions (means). For each region we calculate the number of connected components, its color (RGB), its average size in pixels and its location from the center. We also compute the Shape Width Transform (SWT) as well as a Histogram of Oriented Gradients (HOG) feature vector. Figure 23 shows from left to right KMeans, SWT and HOG algorithms applied to different crops and illustrates these rich feature sets which capture the complicated space of possible images of true targets.

Concatenating all of them gives us the desired feature vectors for training. After training the SVM we use it on the MGS by extracting the crop's features and test it to classify it as a target or non-target. On a simulated dataset of 10k positive targets extracted by MSER and 20k non-targets also found by MSER we trained on 50% and tested on the remaining 50%. The results were a false positive rate of 0.1% and false negative rate of 0.3%. In practice these rates vary but we have seen that the classifier is sufficient for our purposes.

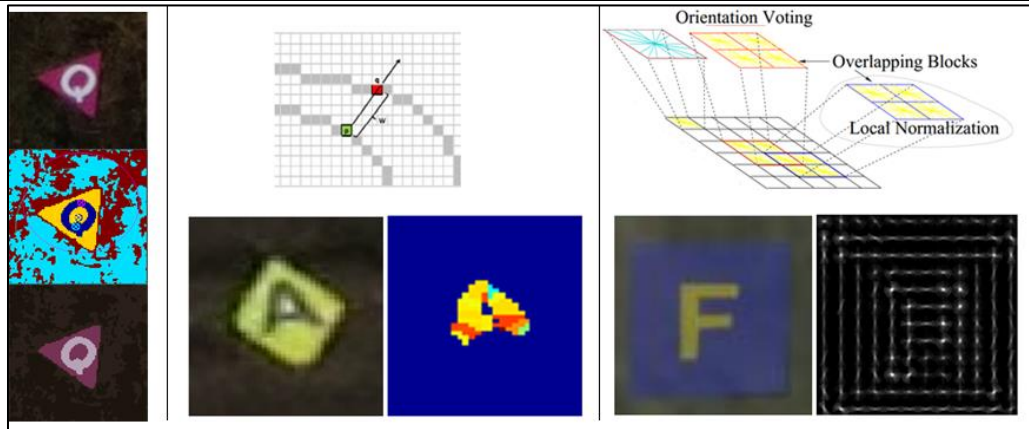


Figure 24 - Left: Detected crop with K-Means centers and reprojected colors. Center: SWT feature extraction process for letter detection. Right: HOG feature extraction process

Color, Optical Character Recognition and Shape

If a crop is classified as a target, getting the letter sign and color is straight forward: the smaller region will be the letter, the next will be the sign and the rest will be the background. Each color is defined by the color centroid and it is compared to a list of colors with mapped names. The letter region is then passed to the alphanumeric classifier and the shape region is passed to the shape classifier.

For alphanumeric classification we use Tesseract which is an open source OCR engine originally developed by HP labs and today supported by Google. It is considered one of the most accurate, flexible and stable open source OCR engines available. Alphanumeric classification and orientation detection are done simultaneously in the workflow. Given a binarized version of the letter segment as well as its orientation information from the UAV, we would like to orient the segment and then see if we can recognize any alphanumeric character in one of its 8 forms of orientation (N/NE/E/SE/S/SW/W/NW). Using OpenCV functions on the MGS and Tesseract APIs we rotate the segment and run OCR on every iteration which returns a character (if found) and a confidence level. Then the algorithm determines the most likely character and returns it with the orientation it was found in. This process is visualized in Figure 24.

The shape classification algorithm uses binary closing to slightly improve the smoothness of the shape contour and then applies OpenCV's convexityDefects function to count the number of edges for shape classification. Additionally an ellipse is fit to the shape outline to determine whether a portion of the shape is circular or elliptical. All this information is used to make a final decision for each target on its properties in a fully automatic fashion without any interaction from the user.

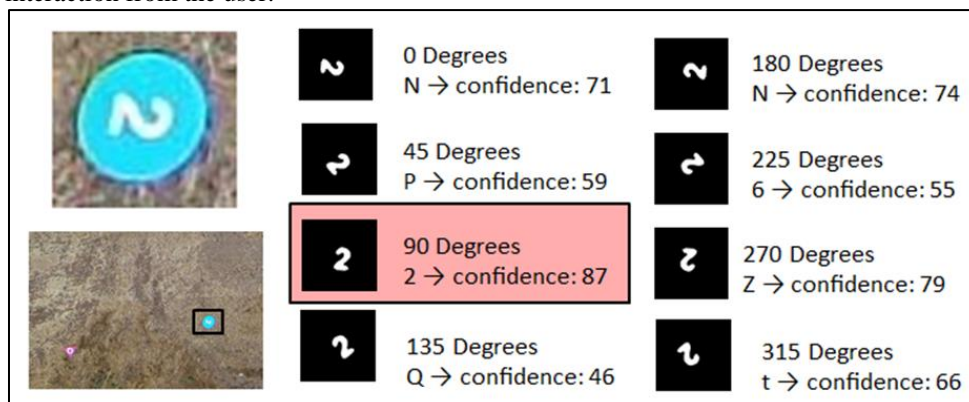


Figure 25 - OCR and orientation detection process using the Tesseract engine. The binarized letter mask from K-Means is rotated in 8 orientations and the strongest scoring orientation and letter is chosen.

2.5 Mission Ground Station (MGS)

The Grey Owl MGS can be broken into two functional capabilities, completely independent from each other and separated on both the hardware and software levels:

1. Flight management console – consisting of the RFD900 communication module, egg-drop calculating algorithm and the dedicated ground tool of the APM 2.6 autopilot, "APM Mission Planner".
2. Target identification consoles – consisting of the Nanostation communication module and a custom software utilizing automatic detection and management of the captured targets as mentioned in the previous section.

Several Mission Ground Station applications compatible with the APM autopilot were examined during ground testing and simulations before the "APM Mission Planner" was chosen. Although most of them covered similar functionalities, the mission planner gains the advantage in overall reliability and minimized crew workload.

Extensive flight testing proved the mission planning tools met all expectations, airframe tuning to be intuitive and its Flight Data tab (shown in the figure below) to allow efficient situational awareness while providing advanced monitoring capabilities and control of the Grey Owl UAV.



Figure 26 - Flight Data tab of the APM Mission Planner

2.6 Air Drop Task

Preparations for the Air Drop Mission were conducted in 3 main steps: Simulations, Wind tunnel testing and Ariel drops. A Monte Carlo Simulation was performed with control over several parameters affecting the egg-ribbon trajectory: mass, attitude, angular velocity, drag coefficient, initial height and plane velocity. The sensitivity of each parameter to error meas. and variable wind speed (modeled as a Weibull distribution based on data from weather.com of the competition area) and direction was studied by fixing the variables under inspection and running the simulation at up to 10^5 iterations. It was found that the projectile mass and initial height were most important for better clustering and accuracy.

A wind tunnel test was done in order to measure the drag coefficient of the egg-ribbon structure. The results were incorporated in the script used to calculate the impact point during the flight. The impact location was calculated using real time telemetry: air speed, wind speed, GPS coordinates and attitude and angular velocity, then solving the equations of motion for the impact location:

$$\dot{\vec{x}} = \vec{a}_{gravity} + \vec{a}_{drag} = (\dot{x}, \dot{y}, \dot{z}, x, y, z) \quad ; \quad \vec{a}_{gravity} = (0, 0, -g)$$

$$\vec{a}_{drag} = -\frac{1}{2} \rho A C_d |\vec{V}| \vec{V} = -\frac{1}{2} \rho A C_d \sqrt{(\vec{v}_{egg} - \vec{v}_{wind})^2} (\vec{v}_{egg} - \vec{v}_{wind})$$

The algorithm used for the egg's release:

If: Manual authorization **AND** Airspeed > 25kts **AND** 300ft < Altitude < 400ft **AND** UAS Location < 200ft from target **AND** Projected impact location is inside the wanted area \Rightarrow Release

Ariel tests were performed during the entire flight testing phase, while the script was improved to allow for the system delay time. Initially with manual drops, and finally with the algorithm above using a python script which was integrated in the autopilot firmware, calculating an impact point with a refresh rate of 35Hz. This process eventually resulted in a success rate of more than 80% for hitting within 50ft from the target location.

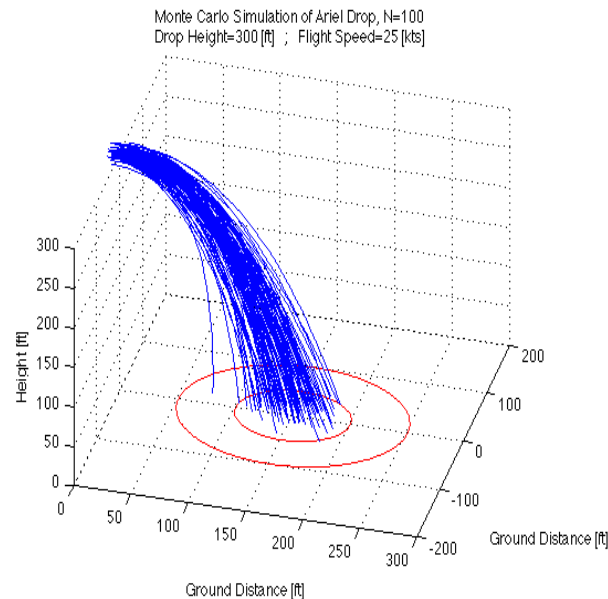


Figure 27 – 3D trajectories showing the results of the Monte Carlo Simulation of an Ariel Drop

3 Flight Testing, System Verification & Airworthiness

3.1 Mission Task Performance

Advancement of the Grey Owl system progressed on two fronts—building and experiments. System integration is where these fronts overlap; a sort of feedback control between the intended input (building) with the actual results (experiments). This integration often took place in the faculty workshop, where systems that had just been assembled could be immediately tested and verified.

While these tests were important, there could be no substitute for actual flight experiments. These experiments represented a huge investment of effort from the team and often taking up the better part of a day and executed weekly throughout the year given the system was in operable condition.

In order to test and evaluate the Grey Owl system as soon as possible, the team designed and built a wooden ‘demonstrator’ model immediately after finalizing the aircraft’s preliminary design. The demonstrator’s maiden flight took place just two months after the first project meeting, giving the team the ability to test performance at each stage of system development, from a simple RC platform to a fully functional, autonomous UAV that soon met all competition thresholds.

In parallel to system development and mission-competence-evaluation on the demonstrator, work began to design and manufacture the two final, graphite-epoxy airframes. By the time the new UAV’s were ready, the Grey Owl’s mission capabilities had matured significantly. For example, whereas the initial system configuration could only handle around 7 minutes of continuous flight, the UAV’s endurance time increased to 35 minutes. Advancements like these, along with improved Crew Resource Management (CRM), allowed more and more mission tasks to be practiced each flight experiment until the system achieved the desired performance maturity.

3.2 Payload System Performance

Being in the air early was also critical for advancement of the system’s target recognition algorithms, as well as for selection and integration of the imagery payload configuration. Special emphasis was placed on building an aerial image database of targets the team had made and spread throughout the airfield each flight experiment in accordance with competition mission specifications. This growing database allowed the image recognition algorithms to be developed and checked, not only in real-time, but back at campus as well.

3.3 Guidance System Performance

The development of the Grey Owl’s guidance system began with system-level verification of sensor & estimation performance, both on campus and airborne. The Ardupilot’s Kalman filtering (recently upgraded to Enhanced Kalman filtering) process and adequate sensor errors were found to produce accurate and consistent guidance performance, exceeding the requirements specified in chapter 2.2.

After a methodical PID control calibration process was conducted to fit the APM to the Grey Owl airframe and extensive flight testing, superb and reliable autonomous capabilities were achieved. Effort was then focused on training various navigation scenarios in order to efficiently carry out all mission tasks.

3.4 Evaluation Results

Missions	Evaluation
Autonomous Flight Task	Performed over 105 successful flights consisting of more than 10 hours of flight time, 7 of which were strictly autonomous.
Search and Identify Targets	Successful target recognition and characteristic identification.
Automatic Detection, Localizing and Classification	Adequate automatic detection capabilities with less than 40% False Alarm Rate (FAR).
Actionable Intelligence	Successful real-time target identification.
Off-Axis Target	Successful tracking and manual identification at 630 feet of a target placed 700 feet from the flight path.
SRIC	Large file size transfer carried out successfully at a range of 1500ft and a mission time of 45 seconds.
Emergent Target	Successful real-time identification of human targets.
Interoperability	Successful real-time task simulation.
Air Drop	Performed over 20 manual airdrops, 15 calculated autonomously, with an average impact deviation of 35 feet

Table 7 - Evaluation Results

4 Safety Considerations / Approach

4.1 Specific safety criteria

In order to successfully develop a fully functional unmanned system, emphasis on safety was essential. During the design, manufacturing and verification of the Grey Owl UAS, continuous risk assessments were carried out in order to minimize possible harm of personnel and property. These assessments dictated design restraints, guided team operational policies, and included:

- Establish safe workshop activity protocol
- Proper flight line communication and separation.
- External engine cut-off apparatus.
- Short term failsafe (Return To Launch)
- Flight termination in case of excessive communication time-out
- Installation of a Dual Receiver Unit which separates the RC Receiver and autopilot on the hardware level (manual control and servo operation is retained in the event of an autopilot failure).

4.2 Safety risks and mitigation methods

Checklists were developed and expanded as needed throughout the year for inventory, safety procedures, and pre-flight readiness procedures. In addition to general procedures, the specific goals and guidelines of each experiment were prepared and reviewed both in advanced and as a team immediately before each flight.

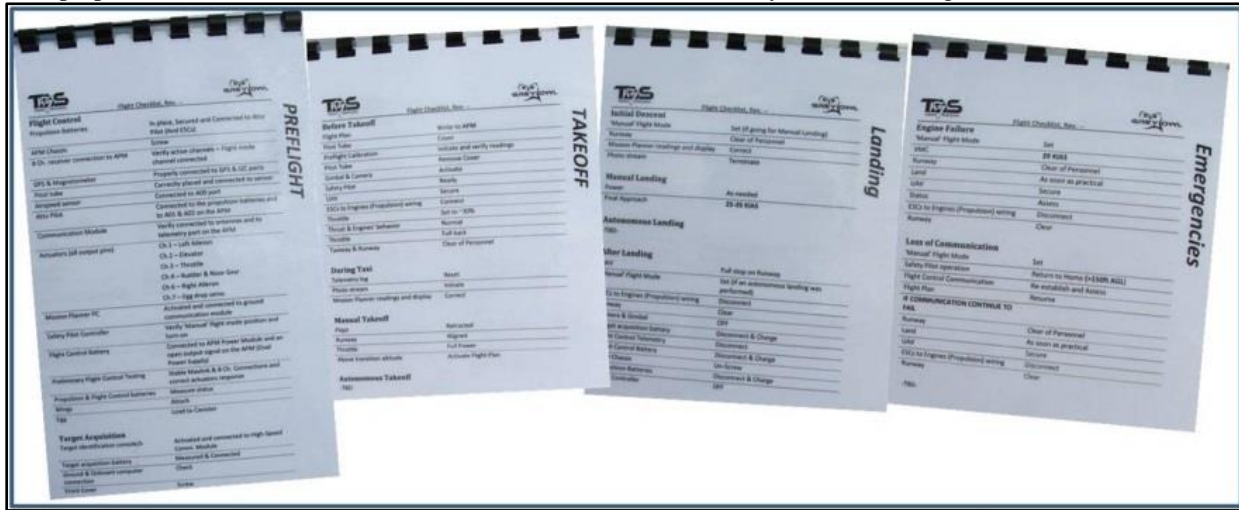


Figure 28 - Grey Owl team's checklists

While each experiment had intended, detailed guidelines, the team quickly became adept at dealing with unforeseen setbacks, such as calibration errors, engine failures, or integration issues. Despite being first-year competitors, the team's ability to handle problems quickly grew, often involving several dedicated hours back at the faculty workshop running system diagnostics, performing thrust tests with variable isolation, digging through and analyzing telemetry logs, researching issues on forums or consulting advisors. Each setback, while straining the project's timeline, invariably resulted in improved system performance and team knowhow.